Journal of Thermal Analysis, Vol. 36 (1990) 1141-1153

THERMAL DECOMPOSITION OF ANTIMONY OXYHALIDES
I. Oxychlorides

L. Costa, G. Paganetto**, G. Bertelli*** and *G. Camino*.*

*DIPARTIMENTO DI CHIMICA INORGANICA, CHIMICA FISICA E CHIMICA DEI MATERIALI, VIA P. GIURIA 7, 10125 TORINO, ITALY
**"HIMONT ITALIA S.R.L.", CENTRO RICERCHE "GIULIO NATTA", P. LE DONEGANI 12, 44100 FERRARA, ITALY.

(Received October 23, 1989)

The thermal decomposition of SbOCl, $Sb_4O_5Cl_2$ and $Sb_8O_{11}Cl_2$ has been studied by thermogravimetry with identification of the products resulting in the condensed phase by X-ray diffraction and infrared technique. It is shown that in nitrogen SbOCl undergoes progressive stepwise thermal disproportionation to Sb_2O_3 and $SbCl_3$ with formation of $Sb_4O_5Cl_2$ and $Sb_8O_{11}Cl_2$ and as intermediates. It is thus confirmed that Sb_3O_4Cl, suggested to be formed instead of $Sb_8O_{11}Cl_2$, is not an intermediate of this process. An identical mechanism is observed in air but with oxidation of Sb_2O_3 to Sb_2O_4.

Antimony oxyhalides are key products in Sb_2O_3-halogenated compounds fire retardant mixtures [1]. Indeed, it is generally proposed that in these systems antimony oxyhalides are formed on heating which would give the flame poison antimony trihalide by further thermal decomposition. However, conflicting data are reported in the literature as to their decomposition process. For example two different schemes have been proposed for the progressive stepwise thermal disproportionation of SbOCl to $SbCl_3$ and Sb_2O_3 through oxychlorides characterised by decreasing Cl/Sb ratio [2-4]. Belluomini *et al.* [2] proposed a sequence involving $Sb_4O_5Cl_2$ and $Sb_8O_{11}Cl_2$:

$$5\ SbOCl\ (s) \xrightarrow{190-240^{\circ}} Sb_4O_5Cl_2\ (s) + SbCl_3\ (g) \qquad (1)$$

$$11\ Sb_4O_5Cl_2\ (s) \xrightarrow{390-460^{\circ}} 5\ Sb_8O_{11}Cl_2\ (s) + 4\ SbCl_3\ (g) \qquad (2)$$

$$3\ Sb_8O_{11}Cl_2\ (s) \xrightarrow{470-540^{\circ}} 11\ Sb_2O_3\ (s) + 2\ SbCl_3\ (g) \qquad (3)$$

John Wiley & Sons, Limited, Chichester
Akadémiai Kiadó, Budapest

Whereas Pitts *et al.* [3] suggested the formation of Sb_3O_4Cl instead of $Sb_8O_{11}Cl_2$:

$$5\ SbOCl\ (s) \xrightarrow{245-280^{\circ}} Sb_4O_5Cl_2\ (s) + SbCl_3\ (g) \qquad (4)$$

$$4\ Sb_4O_5Cl_2\ (s) \xrightarrow{410-475^{\circ}} Sb_3O_4Cl\ (s) + SbCl_3\ (g) \qquad (5)$$

$$3\ Sb_3O_4Cl\ (s) \xrightarrow{475-565^{\circ}} 4\ Sb_2O_3\ (s) + SbCl_3\ (g) \qquad (6)$$

Both groups support their scheme on the basis of thermogravimetric data with, however, an apparently better agreement between calculated and experimental weight loss reported by Belluomini *et al.* [2] (Table 1). In addition, previous evidence of the existence of Sb_3O_4Cl (e.g. Ref. 5) seems to have been subsequently disproved [2, 6-8]. In this paper the thermal behaviour of antimony oxychlorides is assessed by combining thermogravimetric data with identification by X-ray diffractograms (XRD) and infrared spectra (IR) of the products of decomposition.

Experimental

Materials

Antimony oxides. Samples of the two allotropic forms of Sb_2O_3 stable at room temperature: dimeric, cubic senarmontite and polymeric, orthorombic valentinite [9, 10] were supplied by Associated Lead (Timonox White Star) and C. Erba, respectively. The purity grade was better than 99 %. Cervantite, alpha-Sb_2O_4 was prepared by heating senarmontite to 650° in air. IR and XRD patterns of the three oxides shown in Fig. 1 and 2 respectively, are in agreement with published data, e.g.: IR ref. 9, 10; XRD ref. 11, card n° 5-0534 (senarmontite), n° 11-689 (valentinite), n° 11-694 (cervantite).

Antimony oxychlorides. The preparation by hydrolysis of analytical grade $SbCl_3$ (C. Erba) was carried out following the procedures described in ref. 12 for SbOCl and by Belluomini *et al.* [2] for $Sb_4O_5Cl_2$ and $Sb_8O_{11}Cl_2$. XRD patterns are in good agreement with those calculated on the basis of Ref. [11] for SbOCl and $Sb_4O_5Cl_2$ (Fig. 3 and 4). Whereas repeated accurate attempts to prepare $Sb_8O_{11}Cl_2$ by the published procedure [2] gave a product of poor crystalline quality as shown by Fig. 5a. Comparison with published data (Fig. 5b) shows similarity only for the most intense peak (2θ = 27.6 - 27.9), whereas the relative intensities of the other peaks are generally dif-

Table 1 Weight loss percent (WL) in TG of SbOCl

Step	Fig. 7		Ref. 2*		Ref. 3**		Ref. 7***		Calculated WL for reactions	
	T, °C	WL	T, °C	WL	T, °C	WL	T, °C	WL	(1-3)	(4-6)
1	270-275	26.5	190-240	25.8	245-280	24.1	220	26.4	26.3	26.3
2	405-475	9.5	390-460	9.1	410-475	8.4	410	9.7	9.6	6.9
3	475-570	11.0	470-540	7.5	475-565	9.5	530	-	8.0	10.6
4	570-675	51.5	>540	-	565-658	54.3	-	-	56.1	56.1

* Heating rate 5 deg/min; nitrogen 50 cm^3/min

** Heating rate 10 deg/min; argon 80 cm^3/min

*** Temperature at which decomposition begins, heating rate 6 deg/min; nitrogen.

ferent. IR spectra shown in Fig. 6 agree with those reported in the literature in the case of SbOCl [13, 14] and $Sb_4O_5Cl_2$ [14] whereas that of $Sb_8O_{11}Cl_2$ was not previously reported.

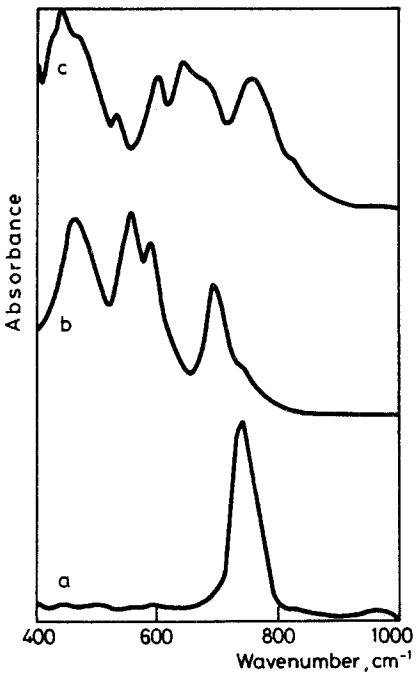

Fig. 1 IR spectra of senarmontite (a), valentinite (b), cervantite (c)

Methods

Thermogravimetry (TG). A Du Pont 951 thermogravimetric analyser 1090 thermal analyser system was used at a heating rate of 10 deg/min under nitrogen or air flow, 60 cm^3/min. Samples of 10-15 mg were held in Pt boats supplied by Du Pont or in home-made silica cylinders (diameter 7 mm, height 7 mm).

Infrared spectra. FTIR spectra of samples dispersed in KBr pellets were obtained on a 1720 Perkin Elmer instrument.

X-ray diffraction studies. XRD patterns were recorded on an Ital Structures diffractometer with Seeman Bohlin geometry and Johansson-Guimier monochromator using CuK_α radiation. ASTM data are reported as "calcu-

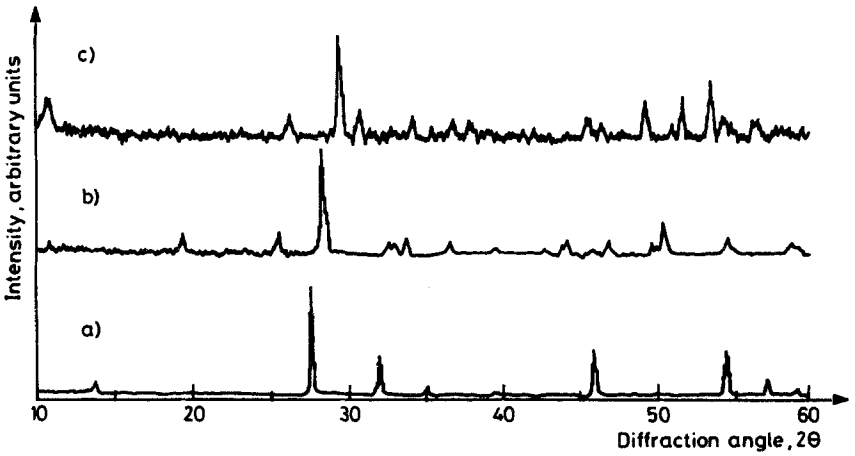

Fig. 2 XRD patterns of senarmontite (a), valentinite (b), cervantite (c)

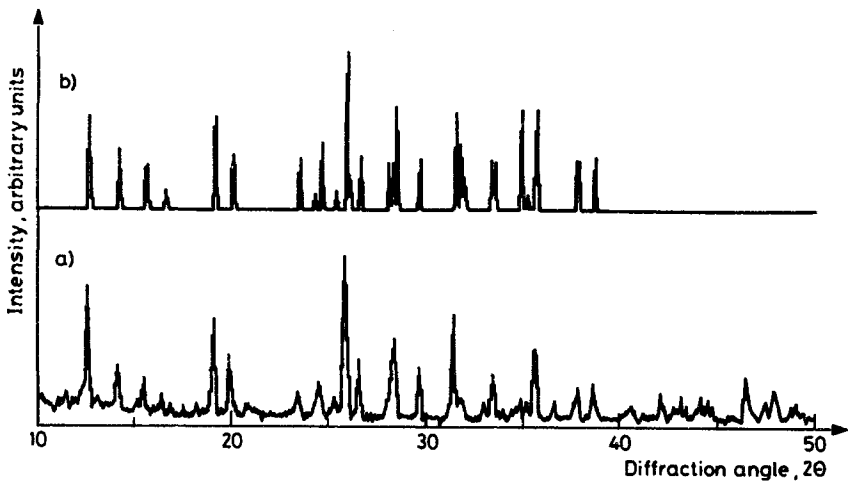

Fig. 3 XRD pattern of reference SbOCl, experimental (a); calculated from ref. 11, card n° 9-117 (b)

lated" diffractograms for direct comparison with experimental results. The calculation is based on the sum of Gaussian curves whose position and intensity are those of ASTM powder diffraction file while the width is as-

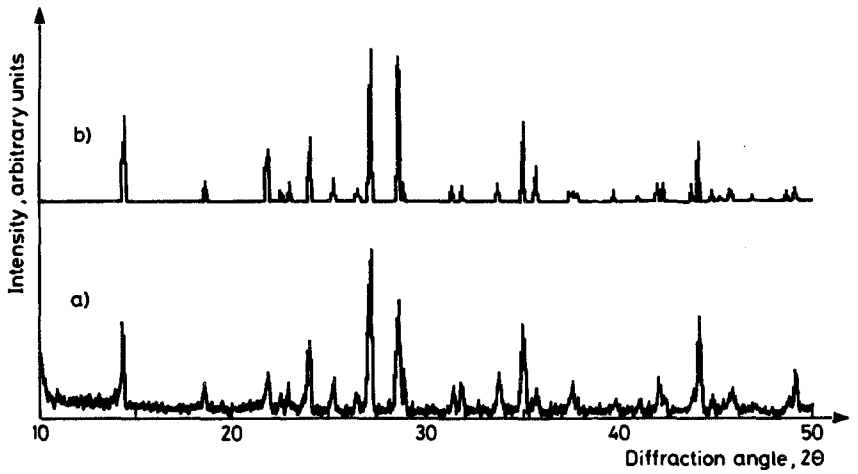

Fig. 4 XRD pattern of refernce $Sb_4O_5Cl_2$, experimental (a), calculated from ref. 11, card n° 30-91 (b)

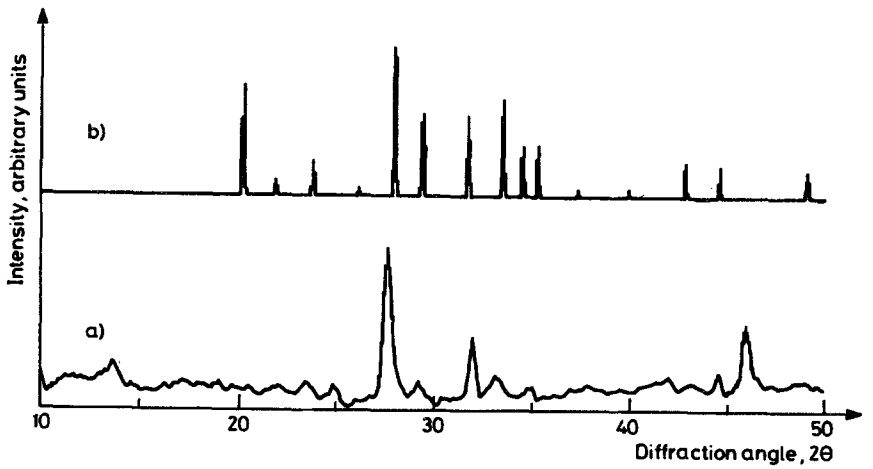

Fig. 5 XRD pattern of refernce $Sb_8O_{11}Cl_2$, experimental (a), calculated from ref. 11, card n° 21-52 (b)

signed from the average found for corresponding diffraction peaks of our products.

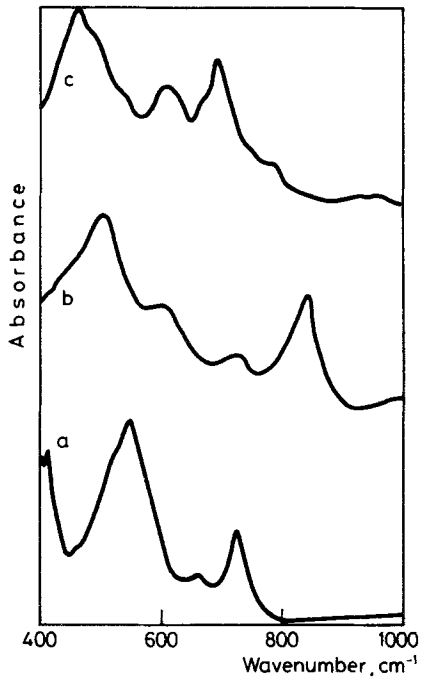

Fig. 6 IR spectra of reference SbOCl (a), $Sb_4O_5Cl_2$ (b), $Sb_8O_{11}Cl_2$,(c)

Results and discussion

Thermal decomposition of SbOCl under nitrogen

The TG and DTG curves of Fig. 7 show that SbOCl undergoes four successive decomposition steps on heating at 10 deg/min between 270 - 675°. The first step occurs at a relatively high rate in a narrow range of temperatures (270 - 275°), whereas successive steps take place over a much larger temperature interval.

The XRD pattern of the product formed at the end of the first step (350°, Fig. 8a) is identical with that of reference $Sb_4O_5Cl_2$ of Fig. 4a with, however, differences as to the relative intensities of some diffraction peaks, e.g. at 2θ = 14.3, 26.9, 28.3, 34.9, 43.8, 48.8. The IR spectrum (Fig. 9a) is comparable with that of reference $Sb_4O_5Cl_2$ (Fig. 6b) showing in particular the absorption at 840 cm^{-1} which is the most typical absorption of this antimony oxychloride. However, different relative intensities are observed for

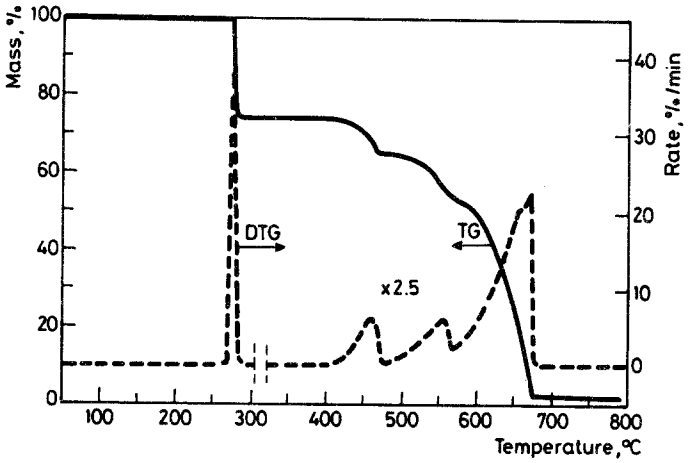

Fig. 7 TG (——) and DTG curves (– – –) of SbOCl; sample pan; Pt; atmosphere: nitrogen, 60cm^3/min; heating rate 10 deg/min

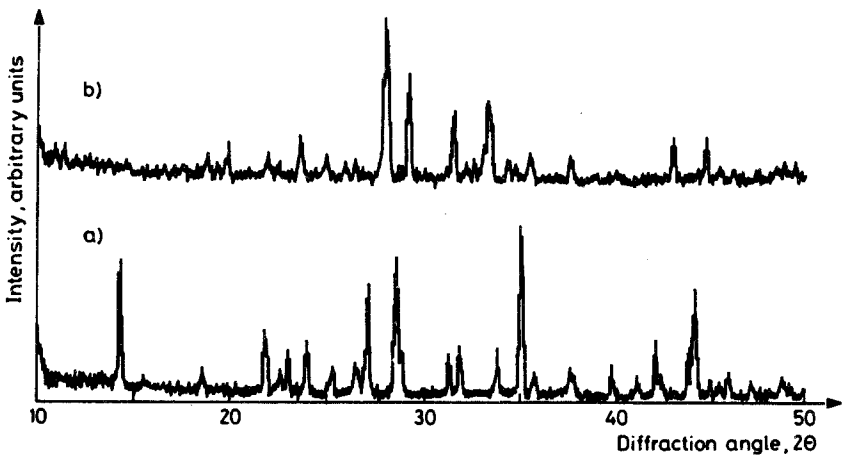

Fig. 8 XRD pattern of the residue from SbOCl heated to 350°C (a) or to 475°C (b)

absorptions at 725 and 600 cm^{-1} in the two spectra and the band at 500 cm^{-1} of reference $Sb_4O_5Cl_2$ is shifted to 515 cm^{-1} in Fig. 9a. On the other hand we have found that, upon heating to 350°, the reference $Sb_4O_5Cl_2$ does not lose weight but shows modifications of original XRD and IR spectrum which become identical to those of Fig. 8a and 9a, respectively. This might be due to a minor heat-induced rearrangement of the antimony and oxygen atoms

which have been shown by structural studies to be organized in a layer structure with antimony-oxygen sheets connected by single chlorine sheets [15].

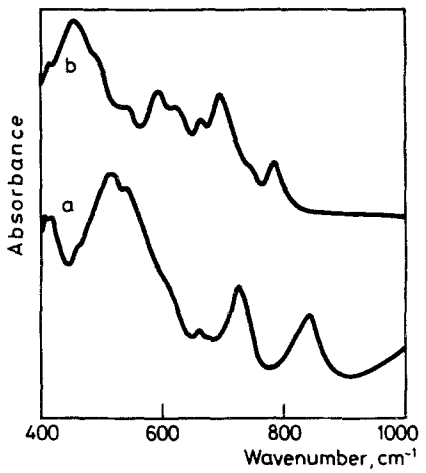

Fig. 9 IR spectra of the residue from SbOCl heated to 350°C (a) or to 475°C (b)

The XRD of the residue of the second step of degradation of SbOCl (475°) shown in Fig. 8b, is almost identical to that calculated from ASTM data for $Sb_8O_{11}Cl_2$ (Fig. 5b) showing a much better crystallinity than the reference $Sb_8O_{11}Cl_2$ prepared by hydrolysis of $SbCl_3$ (Fig. 5a). On the other hand, reference $Sb_8O_{11}Cl_2$ and the residue obtained at 475° from SbOCl show the same IR absorption pattern (Figures 6c and 9b respectively). Indeed the typical absorptions of $Sb_8O_{11}Cl_2$ at 450-460 and 690 cm^{-1} are present in both spectra. However, the spectrum of the product obtained by thermal disproportionation shows better resolution of the absorption bands possibly because of its higher crystallinity. These results agree with those of Matsuzaki *et al.* [16], who found that $Sb_8O_{11}Cl_2$ prepared by hydrolysis of $SbCl_3$ showed poorer crystallinity than that prepared by thermal disproportionation of $Sb_4O_5Cl_2$, giving diffuse X-ray diffraction lines of low intensity.

Finally, XRD and IR studies indicate that the third step of decomposition of SbOCl (475-570°) leaves Sb_2O_3 senarmontite which, in a separate TG experiment, was shown to volatilize above 510° on heating at 10 deg/min. Overlapping of steps 3 and 4 is indeed evident from the DTG curve of Fig. 7. Almost complete volatilization of senarmontite at 675° is shown in Fig. 7 (residue 2%) in agreement with results by Cody *et al.* [9]. Golunski *et al.*

[10] found a residual weight of about 8% at 850° which they attributed to condenaztion of Sb_2O_3 vapors on the balance weighing system. Volatilization of Sb_2O_3 occurs in a two stage process as shown by the shape of the DTG curve in Fig. 7. This behaviour is in agreement with literature data and it was associated with sublimation of senarmontite followed by volatilisation of the melt [9, 10]. Golunski *et al.* [10] showed by DTA that senarmontite heated at 10 deg/min is irreversibly transformed to valentinite at 630-640° which melts at 643-651°. Therefore the two steps of the DTG curve of Fig. 7 with maximum at 660 and shoulder at 650°C should be due to sublimation of senarmontite overlapped by volatilisation of molten valentinite. The relatively low difference between literature data and Fig. 7 (ca. 20°) is normally found when thermoanalytical results obtained with different techniques (i.e. DTA and TG) are compared.

The TG curves of reference $Sb_4O_5Cl_2$ and $Sb_8O_{11}Cl_2$ are similar to the corresponding sections of the TG curve of Fig. 7, that is steps 2-4 or steps 3-4 respectively. In particular, senarmontite was obtained by thermal disproportionation of $Sb_8O_{11}Cl_2$ independently of whether it was prepared by hydrolysis of $SbCl_3$ [2] or by thermal decomposition of reference SbOCl or $Sb_4O_5Cl_2$. This result is in contrast with data by Matsuzaki *et al.* [16] who found senarmontite by heating at 500° $Sb_8O_{11}Cl_2$ obtained by thermal decomposition of $Sb_4O_5Cl_2$ whereas valentinite was formed in the same conditions from $Sb_8O_{11}Cl_2$ prepared by hydrolysis of $SbCl_3$ following the procedure by Belluomini *et al.* [2]. In both cases, these authors also report a complex dependence of the form of Sb_2O_3 on the temperature of heating of the oxychlorides when the temperature is raised from 500° to 590°. The most relevant experimental factor which is different in the present work and in that of Matsuzaki *et al.* is the mode of heating: we have used programmed heating at 10 deg/min whereas Matsuzaki *et al.* used isothermal conditions. This difference, however, seems not to be sufficient to explain the difference in the results.

The experimental weight loss of Fig. 7 and those calculated on the basis of reactions (1-3) and (4-6) respectively can be compared only for steps 1 and 2 (reactions 1 and 2 or 4 and 5) since step 3 (reaction 3 or 6) and step 4 partially overlap in our conditions. On the other hand, the understanding of the reaction occurring in step 2 (reaction 2 or 5) is sufficient to decide between controversial literature data, because the following step depends on the product obtained in step 2. This comparison (Table 1) together with the above identification of the products, confirms that $Sb_8O_{11}Cl_2$ and not Sb_3O_4Cl is the Cl poorest oxychloride obtained on heating SbOCl, in agreement with the reaction scheme proposed by Belluomini *et al.* [2]. Similar

conclusions were reached by Nurgaliev [7] who studied the thermal behaviour of antimony oxychlorides prepared by heating Sb_2O_3 with $SbCl_3$.

In this work we observed a slight catalytic effect of Pt of the sample boat on steps 2 and 3 of Fig 7. Indeed, by using the silica sample holder, these two steps occur at a temperature 10-15° higher than in Pt, although the products of reaction and weight losses are the same in both cases. On the other hand we also found that Sb_2O_3 tends to react with silica at high temperature since a residual weight of about 20 % stable above 700° is left when TG of Sb_2O_3 (valentinite or senarmontite) is run using the silica holder whereas in Pt complete volatilization takes place on heating to 675°.

Thermal decomposition of SbOCl under air

The interest of the thermal disproportionation of SbOCl in fire retardant systems requires that this process is also studied under air to simulate fire conditions.

Figure 10 shows that the weight change in four steps takes place in air and in nitrogen (Fig. 7). The weight loss is comparable in the two cases for steps 1-3 in which XRD and IR studies indicate that the same reactions take place. In step 4 a weight loss of about 4.5% occurs in air whereas complete volatilization is found in nitrogen when Pt sample holder is used in both cases. XRD and IR studies indicate that senarmontite is the residue obtained by disproportionation of $Sb_8O_{11}Cl_2$ (step 3, ca 550°) in air and in nitrogen. The residue left in air at 600° shows IR and XRD patterns of alpha Sb_2O_3, cervantite (Fig. 1c and 2c), which is stable up to 1000° [9-10]. Thus, step 4 in air is the result of competition between volatilization of senarmontite and its oxidation to cervantite in agreement with literature data [9-10]. The competition is shifted in favour of oxidation by using the silica sample holder (Fig. 11). In this case the elimination of the catalytic effect of Pt shifts steps 2 and 3 to higher temperature by 15-20°. Therefore it might be that the increase in the rate of oxidation of senarmontite overwhelms that of volatilization.

* * *

This work was carried out with the financial support of the Progetto Finalizzato Chimica Fine II del Consiglio Nationale delle Ricerche.

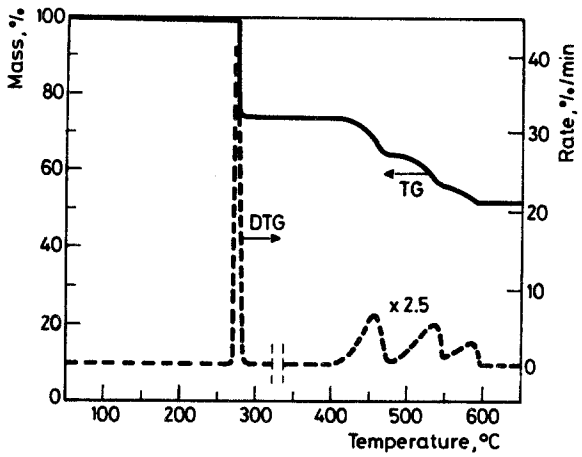

Fig. 10 TG (——) and DTG (– – –) curves of SbOCl, sample pan: Pt; atmosphere: air, 60 cm^3/min; heating rate, 10 deg/min

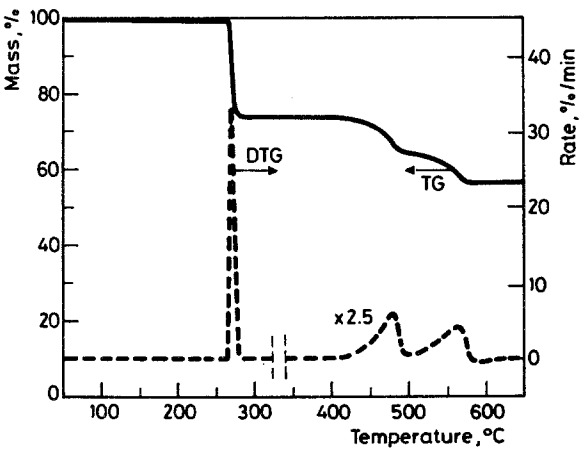

Fig. 11 TG (——) and DTG (– – –) curves of SbOCl, sample pan: silica; atmosphere: air, 60 cm^3/min; heating rate, 10 deg/min

References

1 C. F. Cullis and M.M. Hirschler, The Combustion of Organic Polymers, Clarendon Press, Oxford, 1981.
2 G. Belluomini, M. Fornaseri and M. Nicoletti, Period. Mineral., 36 (1967) 147.
3 J. J. Pitts, P. H. Scott and D. G. Powell, J. Cell. Plastics, 6 (1970) 35.
4 J. W. Hastie, J. Res. Nat. Bur. Stand., 77A (1973) 733.
5 M. Fornaseri, Rend. Acc. Naz. Lincei, 3 VIII (1947) 365.
6 B. Y. Nurgaliev, B. A. Popovkin and A. V. Novoselova, Zhur. Neorg. Kim., 26 (1981) 1043; Russ. J. Inorg. Chem., 26 (1981) 564.
7 B. Z. Nurgaliev, Deposit. Doc. 1981, VINITI 575-82, p. 769; CA 98: 154288k (1983).
8 M. Schulte-Kellinghaus and V. Kramer, Experientia, Suppl. (1979) 37 (Angew. Chem. Thermodyn. Thermoanal.), 29.
9 C. A. Cody, L. DiCarlo and R. K. Darlington, Inorg. Chem., 18 (1979) 1572.
10 S. E. Golunski, T. G. Nevell and M. I. Pope, Thermochim. Acta, 51 (1981) 153.
11 ASTM, X-ray Powder Data File.
12 Handbuch der Präparativen Anorganischen Chemie., G. Brauer, Ed., Verlag, Stuttgart, (1954), p. 465.
13 K. I. Petrov, V. V. Fomichev, G. V. Zimina and V. E. Plyuschev, Russ. J. Inorg. Chem., 16 (1971) 1006.
14 K. I. Petrov, Yu. M. Golovin and V. V. Fomichev, Russ. J. Inorg. Chem., 18 (1973) 1554.
15 M. Edstrand, Acta Chem. Scand., 1 (1947) 178.
16 R. Matsuzaki, A. Sofue and Y. Saeki, Chem. Lett., (1973) 1311.

Zusammenfassung — Mittels TG wurde die thermische Zersetzung von SbOCl, $Sb_4O_5Cl_2$ und $Sb_8O_{11}Cl_2$ untersucht und die entstehenden Produkte der kondensierten Phase mittels Röntgendiffraktionsuntersuchungen und IR-Spektroskopie identifiziert. Es wurde gezeigt, daß SbOCl in Stickstoff einer stufenweise thermische Disproportionierung unterliegt, bei der über die Zwischenprodukte $Sb_4O_5Cl_2$ und $Sb_8O_{11}Cl_2$ zuletzt Sb_2O_3 und $SbCl_3$ entstehen. Es wurde weiterhin bewiesen, daß das anstelle von $Sb_8O_{11}Cl_2$ vorgeschlagene Sb_3O_4Cl kein Zwischenprodukt dieses Zersetzungsvorganges ist. Ein ähnlicher Mechanismus gilt für die Zersetzung in Luft, jedoch mit der Oxidation von Sb_2O_3 zu Sb_2O_4.